ELSEVIER

Tectonophysics 240 (1994) 21–27

TECTONOPHYSICS

Stress distribution over the Mozambique Ridge

Vladimir Lyakhovsky [a], Zvi Ben-Avraham [a,b], Margaret Reznikov [a]

[a] Department of Geophysics and Planetary Sciences, Raymond and Beverly Sackler Faculty of Exact Sciences, Tel Aviv University, Tel Aviv 69978, Israel

[b] Department of Geological Sciences, University of Cape Town, Rondebosch, 7700, South Africa

Received 14 January 1993; revised version accepted 14 December 1993

Abstract

The Mozambique Ridge is an aseismic oceanic plateau in the southwestern Indian Ocean. During the separation of Antarctica and South Africa in the Early Cretaceous, the Mozambique Ridge was segmented by fracture zones which were assumed to become inactive during the Cenomanian, when Africa and Antarctica were finally separated. However, the existence of active normal faulting in the central part of the Mozambique Ridge was demonstrated by single and multichannel seismic surveys. Numerical modelling of the stress distribution caused by the crustal structure of the Mozambique Ridge and the adjacent oceanic basins suggests the possible existence of a zone with average horizontal tension up to 70 MPa along the central part of this passive ridge, which may cause the modern fault activity. These stresses also cause an additional dynamic anomaly which can explain small variations of the geoid anomaly over the ridge.

1. Introduction

About 100 anomalous regions ranging in size from 1000 km down to a few kilometres are located on the world ocean floor. These regions, or oceanic plateaus (Ben-Avraham et al., 1981), are typified by shallow water depth, thick crust, lack of clear magnetic lineations, and steep margins. They cover about 10% of the present-day's ocean floor, with particular concentrations in the western Pacific and the Indian Oceans (Nur and Ben-Avraham, 1982). Oceanic plateaus are aseismic and well embedded within their plates and do not significantly influence the intraplate tectonic processes, except when they reach collisional zones.

One of these aseismic features is the Mozambique Ridge, a large north–south trending oceanic plateau lying roughly parallel to the southeast coast of Africa between 25° and 35°S (Fig. 1). Prior to the formation of the South Atlantic Ocean and the Western Indian Ocean, the Agulhas Plateau and the Mozambique Ridge were attached to Africa (Lawver et al., 1985; Martin and Hartnady, 1986). Recent results of seismic investigations and sampling indicate a continental origin of the southern Agulhas Plateau (Allen and Tucholke, 1981; Tucholke et al., 1981) and the southern Mozambique Ridge (Raillard, 1990; Mougenot et al., 1991). The isostatic response function of the lithosphere beneath the Mozambique Ridge was studied by several authors (e.g., Hales and Nation, 1973; Maia et al., 1990) and all of them suggested a local, Airy type, isostatic equilibrium for the ridge. The geoid anomaly across the Mozambique Ridge (Fig. 2) from global

SSDI 0040-1951(94)00104-H

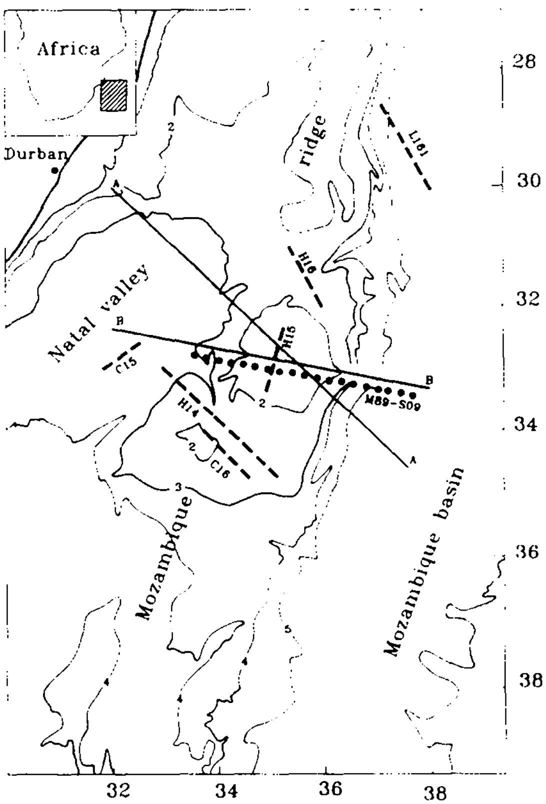

Fig. 1. Bathymetry of the investigated area after Dingle et al. (1987); contour interval 1 km. Solid line $A-A$ = profile investigated by Maia et al. (1990) for the direct geoid modelling (Fig. 2). Dotted line = continuous seismic reflection profile M89–S09 (Fig. 3). Dashed lines = refraction profiles, depth of the boundaries from which were projected on the investigated cross-section $B-B$ (Fig. 4). Inset shows the regional setting.

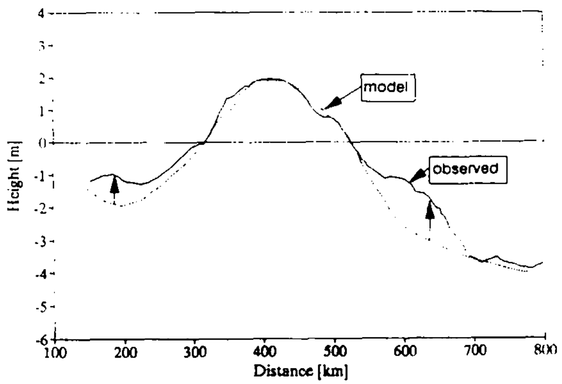

Fig. 2. Computed (dotted line) and observed (solid line) geoid anomaly over the Mozambique Ridge (after Maia et al., 1990). See Fig. 1 for location of profile.

altimetric geoid derived from SEASAT coincides quite nicely with the simulated one, obtained by the 2.5-D direct computation of the geoid anomaly over the ridge (Maia et al., 1990), especially in its central part. However, two local-scale anomalies of about 1–1.5 m amplitude are situated at the transition zones between the continental crust of the ridge and the surrounding oceanic crust.

During the separation of Antarctica and South Africa in Early Cretaceous time the Mozambique Ridge was segmented by fracture zones (Raillard, 1990). These faults became inactive during the Cenomanian, when the continental lithospheres of Africa and Antarctica were finally separated. Since then the Mozambique Ridge is supposed to be a passive feature. However, single and multichannel seismic surveys in this area (Dingle and Robson, 1985; Raillard, 1990) have clearly shown the existence of active normal faulting in the central part of the ridge. In some portions these faults formed asymmetric grabens on top of the ridge (Fig. 3).

The purpose of this paper is to evaluate quantitatively the influence of the crustal structure of the locally compensated oceanic ridge on the horizontal stresses in order to check whether these stresses could produce the active normal faulting on the passive ridge and to evaluate their contribution to the observed geoid anomalies.

2. Geophysical model of the Mozambique Ridge

A density model was calculated along the profile across the Mozambique Ridge (line B–B in

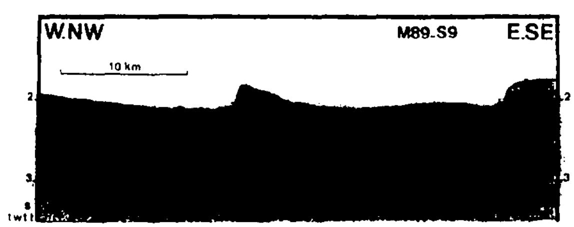

Fig. 3. Continuous seismic profile $M89-S09$ across the Mozambique Ridge (after Raillard, 1990). Note the active normal faults which form half-graben on top of the ridge. See Fig. 1 for location of profile.

Fig. 1), whose location in the central part of the ridge coincides with the seismic reflection line M89–S09 (Raillard, 1990) and perpendicular to the direction of the ridge axis. The geometry of iso-velocity layers was taken from Raillard (1990) and was used as an initial approximation for our

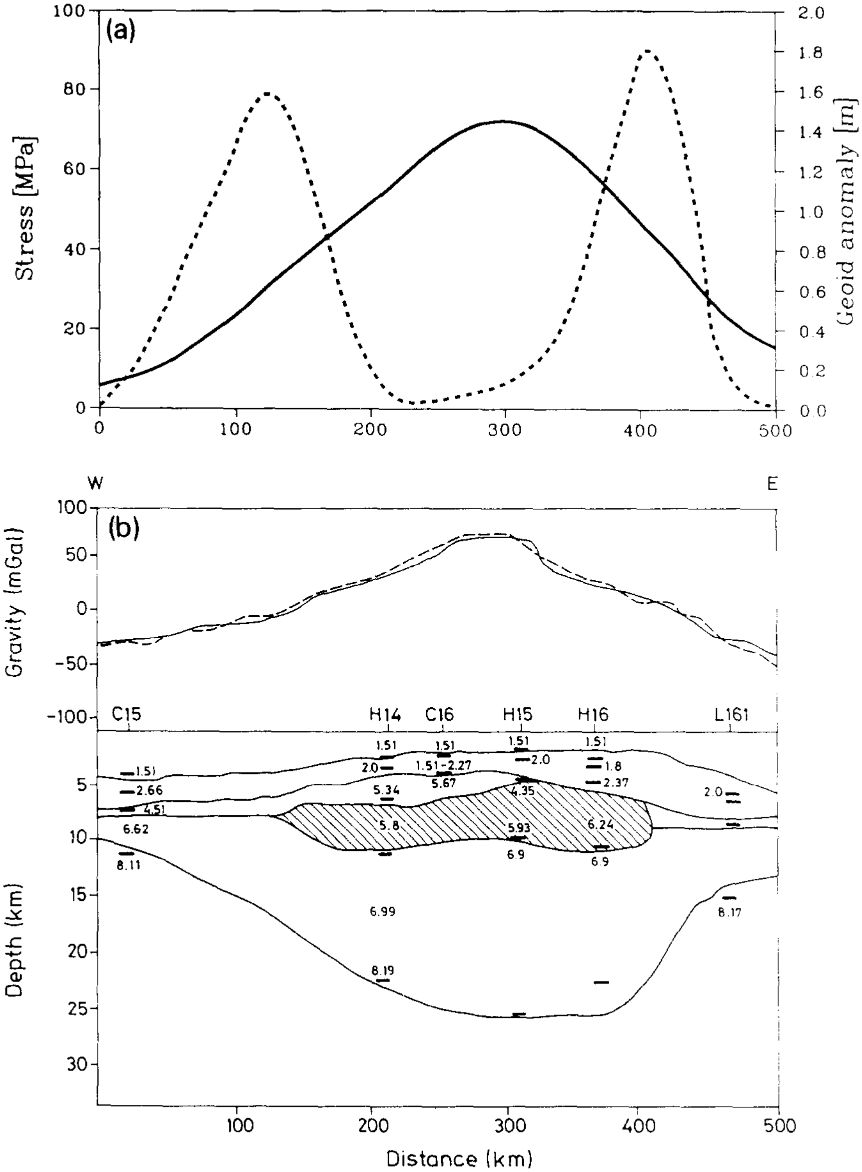

Fig. 4. (a) Simulated average horizontal tension along a profile across the Mozambique Ridge. The maximum tension of about 70 MPa is located in the central part of the ridge where active normal faults exist (solid line). Additional geoid anomalies caused by the simulated stress distribution (dashed line). The simulation is based on the crustal structure shown below. See Fig. 1 for location of profile. (b) Top: free air gravity profile (solid line) across the Mozambique Ridge (Udintsev, 1975) and computed two-dimensional free air gravity anomaly (dotted line) based on crustal model shown. Bottom: model of the crustal structure of the Mozambique Ridge based on gravity and seismic refraction data. Heavy markers correspond to the depth of seismic boundaries from the refraction profiles *C15, C16* (Chetty and Green, 1977), *H14, H15, H16* (Hales and Nation, 1973), and *L161* (Ludwig et al., 1968) projected parallel to the north–south axis of the ridge on the investigated line.

Table 1
Results of density modeling (seismic constraints from Raillard, 1990)

Number of layer	Thickness (km)	Velocity (km/s)	Density (kg/m^3)
1	0.5– 3.0	1.51–2.37	1900
2	0.0– 3.2	4.09–5.67	2200
3	0.0– 6.0	5.80–6.20	2550
4	4.0–15.	6.26–6.99	2920
5	–	8.11–8.19	3100

density model. He suggested that the Mozambique Ridge consists of four main layers. The depths of seismic boundaries from the refraction profiles C15, C16 of Chetty and Green (1977), H14, H15, H16 of Hales and Nation (1973), and L161 of Ludwig et al. (1968) were projected parallel to the north–south axes of the ridge on the investigated profile. The geometry of the layers shown in Fig. 4 is the result of a gravity modelling of the free air gravity anomaly taken from the Geological–Geophysical Atlas of the Indian Ocean (Udintsev, 1975). The range of variations of their thicknesses, seismic velocities and average densities, according to our gravity model, are shown in Table 1.

According to this model the first and the second layers are low- and high-density sediments. Under the high-density sediments there is a layer with a typical granitic velocity. The fourth crustal layer probably represents the lower continental crust. Mass distribution over depth for the density model shown in Fig. 4 was calculated. This calculation suggests that the geometry of the Moho discontinuity (the boundary between layers 4 and 5) fits the local Airy model of the isostatic compensation. The difference between the simulated and observed free air gravity anomaly (Fig. 4) is not more than 10 mGal.

3. Theory

An approximation of the lithosphere as a thin plate lying on an inviscid substratum makes it possible to neglect vertical gradients of the horizontal velocity (e.g., England and McKenzie, 1982, 1983). This means that the horizontal velocity of the lithospheric motion may be represented as a sum of the main components depending only on the horizontal coordinates (x, y) and small perturbations also depending on the vertical coordinate (z):

$$v = v_0(x, y) + \epsilon v_1(x, y, z)$$

where the small parameter $\epsilon = H/L$ is the ratio of the average thickness of the lithosphere (H) to the characteristic length of the investigated area (L). The first approximation of the velocity vector (v_0) describes a vertical average motion of the lithosphere as a whole and allows the deformation of the sheet to be expressed in terms of vertical averages of strain rate and deviatoric stress. Equation of the distribution of the deviatoric stresses (t_{ij}) in the lithosphere with density ρ, relief of the upper boundary S and lower boundary B has the following form (Sonder and England, 1989):

$$\begin{aligned}
&\frac{\partial}{\partial x}\left[(S-B)t_{xx}\right] + \frac{\partial}{\partial y}\left[(S-B)t_{xy}\right] = \int_B^S \frac{\partial}{\partial x}\int_z^S \rho g \, \mathrm{d}z \, \mathrm{d}z' \\
&\frac{\partial}{\partial x}\left[(S-B)t_{xy}\right] + \frac{\partial}{\partial y}\left[(S-B)t_{yy}\right] = \int_B^S \frac{\partial}{\partial y}\int_z^S \rho g \, \mathrm{d}z \, \mathrm{d}z'
\end{aligned} \tag{1}$$

where g is the gravity acceleration.

According to the layered structure of the crust the density may be represented as follows:

$$\rho = \rho_k, \quad \text{for} \quad h_{k+1} \leqslant z \leqslant h_k \tag{2}$$

where h_k is the upper boundary of the layer number k.

Substitution of (2) into (1) yields:

$$\begin{aligned}
&\frac{\partial}{\partial x}\left[(S-B)t_{xx}\right] + \frac{\partial}{\partial y}\left[(S-B)t_{xy}\right] = \rho_1 g h_1 \frac{\partial h_1}{\partial x} + g\sum_{k=2}^{n}(\rho_k - \rho_{k-1})h_k \frac{\partial h_k}{\partial x} \\
&\frac{\partial}{\partial x}\left[(S-B)t_{xy}\right] + \frac{\partial}{\partial y}\left[(S-B)t_{yy}\right] = \rho_1 g h_1 \frac{\partial h_1}{\partial y} + g\sum_{k=2}^{n}(\rho_k - \rho_{k-1})h_k \frac{\partial h_k}{\partial y}
\end{aligned}$$

For the stress distribution along the profile (one-dimensional case) these equations may be solved analytically:

$$t_{xx} = \frac{g}{2(S-B)}\left(\rho_1 g h_1^2 + \sum_{k=2}^{n}(\rho_k - \rho_{k-1})h_k^2 + C\right) \quad (3)$$

where C = constant of integration, corresponding to the level of the regional stress.

At the lower boundary of the lithosphere the vertical components of forces acting on the lithosphere and on the mantle must be equal to each other. Using once more the assumption of a low viscosity of the mantle, the force acting from the mantle on the lower boundary of the lithosphere is equal to:

$$F^{\text{mantle}} = \rho_m g B$$

Here we assumed that the zero coordinate $z = 0$ corresponds to the floating level.

The force acting from the lithosphere on the mantle is:

$$F^{\text{lith}} = \sigma_{zz} n_z + \sigma_{xz} n_x + \sigma_{yz} n_y$$

where n_i is a vector, normal to the lower boundary of the lithosphere.

Due to the non-zero deviatoric stresses the whole vertical stress component σ_{zz} is:

$$\sigma_{zz} = \sum_{z}^{S} \rho g \mathrm{d}z + t_{zz}$$

This means that some additional term must be added to the Airy isostasy equation:

$$\rho_m g B = \sum_{B}^{S} \rho g \ \mathrm{d}z + \delta \quad (4)$$

where:

$$\delta = \sum_{B}^{S} \frac{\partial}{\partial x} \sum_{z}^{S} \frac{\partial}{\partial x} \sum_{z}^{S} \rho g \ \mathrm{d}z_1 \ \mathrm{d}z_2 \ \mathrm{d}z_3 + \sum_{B}^{S} \frac{\partial}{\partial y} \sum_{z}^{S} \frac{\partial}{\partial y} \sum_{z}^{S} \rho g \ \mathrm{d}z_1 \ \mathrm{d}z_2 \ \mathrm{d}z_3$$

This stress distribution produces additional gravimetric and geoid anomalies. From the known correlation between lithospheric stresses and the geoid deviation N (Ricard et al., 1984), it is possible to calculate the geoid anomaly corresponding to the stress distribution:

$$N = -\frac{2\gamma\pi l\delta}{g^2} \quad (5)$$

where $l = S - B$ is the variation of the thickness of the lithosphere; γ = gravitational constant.

4. Results of computer simulation

The gravity model of the Mozambique Ridge allows us to use the approximation of layered structure of the crust in order to calculate the stress distribution. The increase of the crustal thickness and the existence of the low-density granitic layer in the central part of the ridge results in a horizontal tensional stress (Fig. 4). The location of maximum tension of about 70 MPa is in a good agreement with the zone of extension on the Mozambique Ridge.

Recent studies have yielded new insight into the physics and mechanics of the brittle behaviour of rocks (e.g., Evans et al., 1990). However, only a few data on the level of stresses needed for the normal fault formation is available. Calculations based on the observations of joints in granitic rock in the central Sierra Nevada indicate relative tensile stresses of about 1–40 MPa responsible for the fracture formation (Segall and Pollard, 1983). The tectonic stresses corresponding to the normal faulting may be also estimated by the Anderson theory of faulting (Turcotte and Schubert, 1982). Thus, for the most typical friction coefficient $\mu = 0.85$ (Byerlee, 1978) and depth of about 5 km, the angle of dip of a normal fault is $\beta = 65.2°$, and the tectonic stress is $\sigma = 65$ MPa. These estimations suggest that tensional stress of about 70 MPa in the central part of the Mozambique Ridge is probably not enough to create a new fault deeper than 5 km, but it is sufficient to reactivate old faults and cause displacements on their surface.

Variations in stress across elevated regions with large gravity anomalies were analyzed by Lambeck (1980) from consideration of isostasy. This analysis suggests an average value of stress in the crust of these regions of about 50 MPa with maximum values of up to 150 MPa for the Tibetan Plateau. The proposed estimation of the magnitude of the stress for the Mozambique Ridge of about 70 MPa is in agreement with the analysis of Lambeck (1980) for other regions.

In accordance with Eq. (5) the stress field causes additional geoid anomalies shown in Fig. 4. The additional geoid anomalies of about 1-1.5 m are located over the margins of the Mozambique Ridge and can explain the difference between the simulated and observed residual altimetric geoid anomaly (Maia et al., 1990) shown in Fig. 2.

5. Conclusion

Numerical modelling of the stress distribution shows the existence of horizontal tension of about 70 MPa along the central part of the Mozambique Ridge. This tension is caused by crustal structure variations between the locally compensated oceanic ridge and the adjacent oceanic crust. The location of the maximum stress coincides with the location of a zone of active extension in the central part of the Mozambique Ridge. Calculation of additional geoid anomalies caused by this stress distribution makes it possible to achieve a better approximation of the observed geoid anomalies.

Acknowledgements

We thank L. Lobkovsky for the discussion of this work. Critical reading by R. Stephenson, G. Ranalli and C. Ebinger improved the manuscript. M. Rybakov is thanked for providing his programs for 2-D gravity modelling. Work by V. Lyakhovsky was supported by grants from the Israel Ministries of Science and of Absorption and of M. Reznikov by the Israel Ministry of Absorption.

References

Allen, R. and Tucholke, B., 1981. Petrography and implications of continental rocks from the Agulhas Plateau, southwest Indian Ocean. Geology, 9: 463-468.

Udintsev, G. (chief editor), 1975. Geological-Geophysical Atlas of the Indian Ocean. Academy of Sciences of the USSR, main administration of geodesy and cartography under the council of ministry of the USSR, Moscow, pp. 90-91.

Ben-Avraham, Z., Nur, A., Jones, D. and Cox, A., 1981. Continental accretion: from oceanic plateaus to allochthonous terranes. Science, 213: 47-54.

Byerlee, J., 1978. Friction of rocks. Pure Appl. Geophys., 116: 615-626.

Chetty, P. and Green, R.W.E., 1977. Seismic refraction observations in the Transkei Basin and adjacent areas. Mar. Geophys. Res., 3: 197-208.

Dingle, R.V. and Robson, S., 1985. Slumps, canyons and related features on the continental margin off East London, SE Africa (SW Indian Ocean). Mar. Geol., 67: 37-54.

Dingle, R.V., Birch, G.F., Brenner, J.M., de Decker, R.H., du Plessis, A., Engelbrecht, J.C., Fincham, M.J., Fitton, T., Flemming, B.W., Gentle, R.I., Goodlad, S.W., Martin, A.K., Mills, E.G., Moir, G.J., Parker, R.J., Robson, S.H., Rogers, D.A., Salmon, D.A., Siesser, W.G., Simpson, E.S.W., Summerhayes, C.P., Westall, F., Winter, A. and Woodbrorne, M.W., 1987. Deep-sea sedimentary environments around southern Africa (south-east Atlantic and south-west Indian oceans). Ann. S. Afr. Mus., 98(1): 1-27.

England, P.C. and McKenzie, D.P., 1982. A thin viscous sheet model for continental deformation. Geophys. J.R. Astron. Soc., 70: 295-321.

England, P.C. and McKenzie, D.P., 1983. Correction to: A thin viscous sheet model for continental deformation. Geophys. J.R. Astron. Soc., 73: 523-532.

Evans, B., Fredrich, J.T. and Wang, T.-F., 1990. The brittle-ductile transition in rocks: recent experimental and theoretical progress. In: The Brittle-Ductile Transition in Rocks. Am. Geophys. Union, Geophys. Monogr., 56: 1-20.

Hales, A.L. and Nation, J.B., 1973. A seismic refraction study of the Southern Indian Ocean. Bull. Seismol. Soc. Am., 63: 1951-1966.

Lambeck, K., 1980. Estimates of stress differences in the crust from isostatic considerations. J. Geophys. Res., 85: 6397-6402.

Lawver, L.A., Sclater, J.G. and Meinke, L., 1985. Mesozoic and Cenozoic reconstructions of the South Atlantic. Tectonophysics, 114: 233-254.

Ludwig, W.J., Nafe, J.E., Simpson, E.S.W. and Sacks, S., 1968. Seismic refraction measurements on the Southeast African Continental Margin. J. Geophys. Res., 73: 3707-3719.

Maia, M., Diament, M. and Recq, M., 1990. Isostatic response of the lithosphere beneath the Mozambique Ridge (SW Indian Ocean) and geodynamic implications. Geophys. J. Int., 100: 337-348.

Martin, A.K. and Hartnady, C.J.H., 1986. Plate tectonic development of the South West Indian Ocean: a revised reconstruction of East Antarctica and Africa. J. Geophys. Res., 91: 4767-4786.

Mougenot, D., Gennesseaux, M., Hernandez, J., Lepvrier, C., Malod, J.-A., Raillard, S., Vanney, J.-R. and Villeneuve, M., 1991. La ridge du Mozambique (Océan Indien): un fragment continental individualisé lors du coulissement de l'Amérique et de l'Antarctique de l'Est. C.R. Acad. Sci. Paris, Ser. II, 312: 655–662.

Nur, A. and Ben-Avraham, Z., 1982. Oceanic plateaus, the fragmentation of continents and mountain building. J. Geophys. Res., 87(5): 3644–3661.

Raillard, S., 1990. Les marges de l'Afrique de l'est et les zones de fracture associees. PhD thesis, Paris, 272 pp.

Ricard, Y., Fleitout, L. and Froidevaux, C., 1984. Geoid heights and lithospheric stresses for a dynamic Earth. Ann. Geophys., 2: 267–286.

Segall, P. and Pollard, D.D., 1983. Joint formation in granitic rock of the Sierra Nevada. Geol. Soc. Am. Bull., 94: 563–575.

Sonder, L.J. and England, P.C., 1989. Effect of a temperature-dependent rheology on large-scale continental extension. J. Geophys. Res. 94(B6): 7603–7619.

Tucholke, B., Houtz, R. and Barrett, D., 1981. Continental crust beneath the Agulhas Plateau, Southwest Indian Ocean. J. Geophys. Res., 86: 3796–3809.

Turcotte, D.L. and Schubert, G., 1982. Geodynamics. Wiley, New York, NY, 450 pp.